Title: Quiescent horizontal basal stem cells act as a niche for olfactory neurogenesis in a 3D organoid model

Authors: Juliana Gutschow Gameiro[1,2], James E. Schwob[3], Eric H. Holbrook[3,4], Marco Aurélio Fornazieri[1,5**], Brian Lin[3*]

Affiliations:

[1] Department of Clinical Surgery, State University of Londrina, Paraná, Londrina, Brazil
[2] Health Sciences Graduate Program, State University of Londrina, Paraná, Londrina, Brazil
[3] Department of Developmental, Molecular and Chemical Biology, Tufts University Graduate School of Biomedical Sciences, Boston, MA 02111, USA
[4] Department of Otolaryngology-Head & Neck Surgery, Massachusetts Eye and Ear, Boston, MA, USA
[5] Department of Medicine, Pontifical Catholic University of Paraná, Londrina, Brazil

*Corresponding authors: marcofornazieri@uel.br and brian.lin@tufts.edu
Lead contact: Brian Lin

Authors contributions: J.G. and B.L. designed and conducted the experiments; J.S. provided funding; J.G., J.S., E.H., M.F., and B.L. reviewed the data and wrote the paper.

Abstract: The olfactory epithelium contains two basal stem cell populations that facilitate the normally life-long ability for neuronal regeneration that is required for maintaining our sense of smell. Horizontal basal cells (HBCs) are generally quiescent and only become active after direct injury to the epithelium that kills more than just the olfactory sensory neurons (OSNs). Globose basal cells (GBCs) lie apical to HBCs and are solely responsible for the generation of olfactory neurons in the undamaged epithelium. Understanding how these two neurogenic stem cell populations are regulated as OSNs are replenished is hampered by a lack of robust culture models. Here, we report the development of a 3-dimensional organoid model that recapitulates the neurogenic cascade while maintaining both HBCs and GBCs in culture. We use this model to demonstrate that despite their relative quiescence, HBCs form a critical niche for the emergence and composition of the organoid.

Keywords: organoid, olfactory, olfactory epithelium, horizontal basal cell, stem cell, olfaction, neurogenesis, globose basal cell, tridimensional culture.

Introduction:

The mammalian olfactory epithelium (OE) enables our sense of smell through a population of olfactory sensory neurons (OSNs) found in the epithelium, which is normally huge in number and composed of a multitude of odorant receptor-defined types. OSNs are in direct contact with the outside environment, rendering them vulnerable to injury and exhibiting variable lifespans. Accordingly, olfactory neurogenesis is normally lifelong, capable of maintaining the full complement of OSNs and regenerating a normal or near-normal population of neurons after injury. Thus, sensory function can be maintained and even restored, which contrasts with the more limited ability of the central nervous system for regeneration. Underlying the capacity of the OE for robust neurogenesis is the persistence of two multipotent stem cell populations within the OE. Horizontal basal cells (HBCs) lie directly atop the basement membrane and are a dormant population of reserve stem cells. Globose basal cells (GBCs), on the other hand, dwell apical to HBCs and are the active and highly heterogeneous population, including true tissue stem cells, responsible for the homeostatic maintenance of the tissue [1]. The human OE also contains these two stem cell populations and can continually generate OSNs throughout life [2]. However, injuries such as viral infection, exposure to environmental toxins, or even aging itself can compromise the neurogenic process [3–8]. Indeed, our sense of smell diminishes with age, likely through the gradual loss of OSNs and GBCs [3,5,9,10]. No clinically validated therapeutic intervention has yet been developed to treat olfactory dysfunction [11], and this has, in part, been due to the lack of a robust in vitro model of the OE that preserves its cellular and architectural complexities.

In other tissues, the development of tissue-faithful organoids has been the next generation of culture models that have significantly contributed to our understanding of the structure, development, and communication within tissues and mimic in vivo composition and structure [12]. In the OE, prior work used embryonic tissue and purified adult stem cells; however, they do not recapitulate the complexity of the OE in full [13–16]. Here, we establish a robust organoid model of the murine OE that recapitulates adult neurogenesis in vitro and use it to demonstrate that HBCs, despite their own quiescence, act as a necessary niche component for GBCs.

Results:

Previous work has shown that LGR5+ GBCs are multipotent in vivo, that GBCs can be cultured in vitro, and finally, that LGR5+ GBCs embedded in Matrigel can be induced to form organoids [14,15,17,18]. Despite these successes, the structures that were generated in the cultures lacked the characteristic organizational structure found in the OE. We wondered whether the usual interactions between cells *in situ* can function to organize the assembly of a more complex tissue. Accordingly, instead of culturing purified GBCs, we tested whether a combination of the many cell types that exist in the adult tissue could resolve into a more organized structure.

To that end, the olfactory mucosa of adult mice, comprising both OE and the lamina propria was separated from the adjacent respiratory tissue [13] and then dissociated using papain. We reasoned that the fibroblasts of the lamina propria might overtake the epithelial cells in culture, so we discarded those cells that had adhered to tissue culture plastic within 1 hour of plating and cultured the remainder in media containing WNT signaling components [17,19,20].

By day 6 in culture, neurite-like projections emanated from 3-dimensional structures that were attached to the bottom of the well (Fig. 1A). Given the appearance of these projections, we immunostained for canonical markers of olfactory sensory neurons (GAP43, UCHL1, and TUBB3A/Tuj1), as well as those characteristic of GBCs (SOX2, NEUROD1) and HBCs (KRT5) (Fig. 1B-1F). The immunostaining reveals organoids contain HBC-like cells (KRT5+/SOX2+) associating with upstream GBC-like cells (KRT5-/SOX2+), neuronally committed/neuron-producing downstream NeuroD1+ GBC-like cells (KRT5-/SOX2+/NeuroD1+), and immature

olfactory sensory neuron (iOSN)-like cells (KRT5-/SOX2-/Tuj+/GAP43+/UCHL1+). Indeed, all the projections emanating from the organoids stain for Tuj1, UCHL1, and GAP43, indicating they were neurites extended from neuron somata.

To confirm the cellular identifications, we performed single-cell RNA sequencing of our organoid cultures and identified 12 distinct cell clusters (Fig. 1G). Unsurprisingly, mesenchymal cells were found in the cultures, along with several distinct *Krt5*+ basal cell populations. Of these, one in particular expressed high levels of the canonical basal cell marker *Trp63*, which we label here as "Trp63 basal". Another basal cell cluster was distinguished by high levels of the squamous marker *Krt13*, which we term "squamous basal." Of note, despite performing stringent microdissection of olfactory epithelium, and explicitly removing the respiratory epithelium, we still recovered ciliated cells (*Foxj1*, *Krt18*), suggesting either they were contaminants through the dissection process or that olfactory stem cells demonstrated plasticity and generated these in our culture model (Fig. 1H). The latter would be consistent with known reports of respiratory metaplasia found deep within the olfactory epithelium after severe injury or with age [3,10,21]. Encouragingly, we also found several clusters of cells that recapitulated the stepwise path of adult neurogenesis found in the olfactory epithelium [1]. Specifically, we identified an actively dividing, Sox2+, Ki67+ multipotent stem GBC population, transitioning into neuronally specified, Ascl1+ GBCs, evolving into Neurod1+ neuronal progenitor GBCs, finally culminating in a Gap43+ immature OSN (Fig. 1I). Thus, besides mature OSNs that require an olfactory bulb for survival, our organoid model contains the full spectrum of cells within the adult neurogenic path in the olfactory epithelium, including quiescent HBCs and active GBCs.

As both multipotent HBCs and GBCs are found in adult OE tissue, the organoids that form in the mixed culture possibly arose from one or both of these cell populations. It is known that GBC numbers increase during regeneration and reduce with age [3,5,10,22]. Thus, we tried to optimize the efficiency of organoid generation in our model using two different approaches: using lesioned OE or adolescent OE as the starting material.

In the first approach, we used methimazole-induced direct OE injury to stimulate the expansion of multipotent GBC stem cells [4,23–25]. OE was harvested and put in the culture at different time points following a single intraperitoneal injection of methimazole and evaluated for the subsequent formation of Tuj1+ OSNs. We found that when OE is harvested at 4 and 5 days after injury, significantly higher quantities of Tuj1+ OSNs were generated when compared with the control (Fig. S2D, $p < 0.05$). To contextualize the results, the dynamics of the stem and progenitor cell populations following methimazole injury were analyzed using immunofluorescence (Fig. S1) and qRT-PCR of a time course following injury (Fig. S2A-C).

We confirmed that methimazole injury ablates nearly all mature cells of the OE by day 1 post-injection. Surprisingly, BSND+ ionocytes (also known as IP3R3+ microvillous cells [26,27]) survived injury and were found interspersed with the remaining HBCs and GBCs even at day 1 post-methimazole. HBCs were the primary proliferating cell population found in the tissue until day 5 post-injury when a basal monolayer of HBCs was reinstated in the OE; at this timepoint, Sox2+ GBCs are the primary proliferating population. The sequential emergence of cell types in situ matched the cell state transition results revealed by the single cell analysis within our organoid cultures: we found that neuronally fated Ascl1+ and Neurod1+ GBCs emerged around day 3 post-injury and reached a maximum by day 5 post-injury. In agreement with our organoid data, 4-5 days post-methimazole injury, there was higher expression of genes for multipotent stem cell (*Lgr5*, *c-kit*, *Trp63*), neurogenic markers (*Ascl1* and *Neurog1*), and the non-neurogenic marker of ionocytes, *Foxi1*.

For the second approach, we tested whether younger adolescent mice, since they have a higher prevalence of stem cell progenitors, including LGR5+ GBCs, would be more efficient at organoid formation [15]. Surprisingly, we found no significant difference in the generation of Tuj1+ OSNs in the cultures formed from tissue harvested from younger mice (Fig. S2E; $p=0.298$).

Though post-methimazole injury conditions produced significantly more Tuj1+ OSNs, we elected to use uninjured adult donor animals for the remainder of the experiments to model normal epithelial homeostasis more accurately. Given the highly suggestive morphology of the HBC "cap" found in many of these organoids, the various HBC-like populations identified in the single-cell RNA sequencing of our cultures and previously published results using only GBCs [17], we wondered whether these HBCs derived from the donor tissue significantly contributed to the organoids. To test this hypothesis, KRT5-CreER;LSL-TdTomato mice were injected with tamoxifen prior to tissue harvest to lineage trace pre-existing HBCs in the starting material and visualize their contribution to the cultured organoids. Strikingly, while HBCs were again found in the vast majority of organoids (85%), lineage-labeled, TdT+ HBCs did not contribute to the neuronal cell populations and remained as HBCs in vitro (Fig. 2). Indeed, during all of our experiments (9 distinct experiments), we observed only a single HBC-derived cell that had differentiated into a non-KRT5+ cell. Finally, we found little or no evidence for dedifferentiation of GBCs into HBCs under these conditions, as 92% of all KRT5+ HBCs were derived from lineage-labeled HBCs.

Despite the complete lack of HBC differentiation in the organoids, their consistent appearance in the majority of organoids led us to hypothesize that they could act as a niche or play some role in the formation of these organoids. To test for a role in the formation of the neurogenic organoids, we mixed purified populations of HBCs with purified populations of neuronally specified GBCs. HBCs were isolated using tamoxifen-induced KRT5-CreER;LSL-TdTomato animals, while Ascl1+ GBCs and Neurog1+ GBCs were isolated on the basis of Ascl1-TdTomato and Neurog1-eGFP signal, respectively. As expected, HBCs, when cultured alone, remained HBCs and did not form any Tuj1+ cells. Ascl1+ GBCs alone produced only a handful of Tuj1+ OSNs, with the majority of cells failing to survive. Surprisingly, in the presence of HBCs, Ascl1+ GBCs produced significantly more Tuj1 immunofluorescence than either cell population alone ($p<0.05$, Fig 3F). Interestingly, Neurog1+ GBCs were incapable of proliferating or surviving, with or without HBC co-culture (Fig 3D-E). This is consistent with Neurog1+ GBCs being a more downstream, limited neuronal progenitor population [28–30].

These experiments, utilizing mixtures of purified cells as starting material, support the hypothesis that HBCs play a role in the formation of the organoids. To determine whether this was mediated through physical contact or secreted factors, we used a transwell system to permit only the free flow of media and soluble factors through the membrane while preventing contact between the different cell types. We seeded dissociated OE on the top layer of the transwell membrane and confirmed that this transwell system supported organoid growth and neuronal differentiation (Fig. 4A and D). In comparison, when we depleted HBCs from the seeded cells using FACS, we observed no differentiation or survival (Fig. 4B and E). However, when HBCs were plated in the bottom chamber of the transwell, we saw a modest rescue of differentiation and survival but not a complete recapitulation of the organoid structures formed when they were physically in contact with each other (Fig. 4C and F). Taken altogether, this suggests that HBCs maintain a niche for neurogenesis through both physical interaction and soluble factors released into the media. Finally, we depleted HBCs from dissociated OE using FACS purification, plated the remainder into standard chamber wells, and found that, indeed, organoids and neuronal differentiation occurred only in the presence of the HBCs (Fig 4 I and J). Thus, in this organoid culture system, HBCs form a niche that regulates GBC survival, maintenance, and neuronal differentiation in both a cell contact- and secreted manner.

Discussion:

The olfactory epithelium, beyond its critical role in maintaining our sense of smell throughout life, is a robust source of two distinct neural stem cell populations. One exhibits all the key markers of dormant reserve epithelial basal stem cells, while the other is highly

heterogeneous and resembles canonical neural stem cells found in the central nervous system [1]. Understanding the complex relationship between these two stem cell populations and what maintains their presence when most other neural stem cells disappear from the CNS and PNS after development would not only impact our ability to develop therapies for the loss of smell (anosmia) but could be a key to understanding and harnessing adult neurogenesis. To this end, many groups have attempted to create in vitro models of the olfactory epithelium in pieces and as a whole. Embryonic tissue has been shown to grow ex vivo, even generating OSNs, while we and others have shown that HBCs and GBCs can be cultured individually [13–15,30]. Even more recently, groups have generated organoid cultures of the OE using selected GBC populations [17,22,31]. These models have significant advantages compared to studying the OE in vivo. However, they all possess critical weaknesses that hamper their use in understanding and harnessing the stem cell dynamics found within the OE – they require hard-to-get, limited tissue samples, cannot expand significantly or only expand purified populations that do not exhibit high differentiation efficiencies, create disorganized or random swaths of cells, or require sorting of relatively rare starting populations.

Here, we describe a 3-dimensional organoid culture that is agnostic to the age of the mouse, requires no purification of starting material, recapitulates the entire neuronal differentiation pathway, and clearly self-organizes, even generating outward axonal projections. Notably, the model does not contain sustentacular or duct/gland cells, as WNT agonism is used explicitly to push the neurogenic fate. While we recapitulated HBC stem cell quiescence in this model, similar to their behavior in vivo, we were surprised to find that they were critical to organoid formation by acting as a niche for the GBCs. Of note, past work studying age-related anosmia in both murine and human tissue demonstrates that GBCs exhaust first, resulting in an aneurogenic/aneuronal OE, that may progress to respiratory metaplasia, potentially arising from the retained HBCs [3,5,9,10,22]. Given our data, along with past observations, we speculate that the OE might maintain a nearly lifelong neurogenic capacity through the delicate balance of these two disparate stem cell populations, and disease or aging may dysregulate this balance. While elucidating these mechanisms would be difficult in vivo, our new in vitro model enables us to not only perform complex genetic and small molecule manipulations but also reconstitution assays. The mixing experiments reported here are an example of the power of the reconstitution assay, which has yielded a novel model of the OE demonstrating the interdependence of the two adult neuro-competent stem cells. Furthermore, an extension of this platform to human brush biopsies would allow toxicity testing, disease modeling, aging, and testing treatments. Future work will be needed to extend this model to human tissue, improve the efficiency and passaging of organoid culture, identify the conditions necessary for stable maturation of OSNs, and identify conditions that support co-induction of the other cell types of the OE. Our single-cell RNAseq data also demonstrates a high level of heterogeneity in the KRT5+ basal cells found in our culture. Whether this represents a previously unappreciated level of true heterogeneity that is made detectable in tissue culture or is a tissue culture artifact remains to be seen. Finally, based on our identification that quiescent HBCs appear to form a niche for GBCs, it remains to be seen whether GBCs, in return, provide a neurogenic niche for HBCs and whether this interplay exists in vivo.

Materials and Methods:

Animals

Wild-type adult C57/BL6 mice (WT) were purchased from Jax, stock #000664, and used for the organoid characterization experiments. Wild-type adult CD1 mice (CD1) were purchased from Charles River, stock #022, and used for the methodology improvement experiments (aging and methimazole). Animals of both sexes were used in nearly all the experiments and were generally between 6-16 weeks of age. The only exception to this was in the methodology optimization experiments where all mice were male and between 3-6 weeks old. All mice were maintained following IACUC guidelines, with ad libitum rodent chow and water. The heat and humidity were controlled with a 12:12 hour light-dark cycle. The Committee approved all protocols using animals for the Humane Use of Animals at Tufts University School of Medicine.

K5-CreER^{T2} (K5^{CreERT2}), transgenic mice that were generously provided by P. Chambon via R. Reed [32], were bred to the Cre reporter (B6.Cg-Gt(ROSA)26Sortm9(CAG-TdTomato)Hez/J; stock #007909, which expresses Tdtomato in HBCs after tamoxifen administration [33]. Ascl1-TdTomato mice were in-house [34], MMRRC 043552, and expressed TdTomato in the Ascl1+ GBC stage. Neurog1-GFP BAC transgenic mice generated through the GENSAT Project were obtained from Jackson Labs, stock #017306 [35]. Ascl1-TdTomato; Neurog1-eGFP dual reporter mice were obtained by breeding the Ascl1-TdTomato and Neurog1-eGFP mice together to simultaneously label the upstream Ascl1+ GBCs and the downstream Neurog1+ GBCs.

Tamoxifen (diluted in corn oil, 20mg/ml, CAS 8001-30-7, Spectrum® Ref. CO136, Lot. 2KA0296) was injected intraperitoneally at 150mg/kg, and tissue was collected 5-7 days after tamoxifen injection. Methimazole (CAS: 60-56-0, diluted in PBS at 10 mg/ml) was injected intraperitoneally at 50 mg/kg, and tissue was collected between 1 and 14 days to obtain a time course.

Tissue processing for cell culture

The animals were euthanized by CO_2 inhalation, followed by a transcardiac flush of 10-20ml of 1x PBS (pH 7.4). The olfactory epithelium was harvested from the septum and both turbinates, avoiding the respiratory epithelium [13]. Tissue was minced in 500µL of HBSS 1X (with calcium chloride and magnesium chloride, Gibco ref. 24020-117) before 500 µl of Papain (40U/ml in EBSS) and 500 µl of activation buffer (0.067 mM beta-mercaptoethanol, 1.1 mM EDTA, 5.5 mM Cystein-HCl, in EBSS) was added to the tissue and incubated for 30 minutes with agitation at 37°C. Samples were filtered through a 40µm mesh, pelleted at 500g for 5 min), and washed twice with HBSS 1x or DMEM/F12 1x (with 1x primocin and Y27632 10µM, Gibco® ref. 11320-033, lot. 2522615). The final pellet obtained was resuspended and cell-sorted or went straight to culture after counting. All steps are done on ice and performed as quickly as possible to avoid cell death.

Tissue processing for sections

The animals were euthanized by CO_2 inhalation, followed by a trans cardiac flush of 10-20ml of PBS 1x (pH 7.4) and 20 ml of fresh, ice-cold 4% paraformaldehyde. The nose was dissected, and the turbinates and septum were kept together. The tissue was kept in 4% PFA under vacuum for 1 hour, followed by a wash with PBS 1x and left overnight in decalcification solution (Saturated EDTA, 4ºC). The tissue was washed and left overnight in 30% sucrose and frozen in Scigen Tissue-Plus™ O.C.T. Compound (#23-730-571) using liquid nitrogen. Samples were stored at -80ºC until they were cut into 12µm coronal sections on a Leica cryostat.

Bulk RNA isolation

The animals were perfused with 10 ml of PBS1X and the nasal turbinates were dissected on ice, then They were homogenized with 500 µL of Trizol. After 100µL of Chloroform was added

and vortex. After incubation of 3 minutes in RT, it was spun down for 10-15 min for debris separation, and the supernatant was collected. RT incubation of 5 to 10 minutes after the addition of 300µL of RNAse-free isopropanol was done and another spin (30 minutes, 4ºC, 500g). The pellet was washed with RNAse-free 70% ethanol and resuspended in DEPC-treated water. cDNA was generated using Invitrogen SuperScript IV VILO Master Mix with ezDNase (#11766050) following the manufacturer's instructions.

Fluorescence-activated cell sorting (FACS)

Flow cytometry was performed on a FACS Aria II (BD Biosciences). Debris was excluded using forward and side scatter area and doublets were excluded using a stringent two-step gating based on forward and side scatter height versus width. Fluorescence-minus-one (FMO) controls guided gating schemes. Negative controls were used to gate away autofluorescence. The $K5^{CreERT2}$ + HBC population and Ascl1-TdTomato GBC population were selected by the Tdtomato signal, and Neurog1-eGFP+ GBCs by the FITC signal. CD54/ICAM-1 sorting of HBCs was assessed and yielded non-viable HBCs, likely due to the blocking nature of the antibody on a surface adhesion receptor (data not shown).

Cell culture

Dissociated olfactory epithelial tissue was either FACS purified or plated into a tissue-culture-treated plate in DMEM/F12 media containing primocin for 1 hour to remove fibroblasts. Afterward, the supernatant was collected, centrifuged, and diluted in DMEM/F12 media before counting and plating into chambers. Depending on the conditions used, different cell numbers were used per chamber (2 wells: Lab-Tek #177380; 8 wells: Lab-Tek #177402; 4 wells: Lab-Tek #177399 or 8 wells: NEST #230108; 4 wells: NEST #230104), the specific cell number used for each experiment are described below.

For standard organoid culture and immunostaining, we used wild-type mice and plated 75,000 cells per well of an 8-well chamber slide. For single-cell RNAseq, 1.5 million cells were plated into 2-well chambers. For lineage trace experiments using $K5^{CreERT2}$ lineage-traced mice, 75,000 cells were plated per well of an 8-well chamber slide. For the reconstitution experiments, 10,000 FACS-purified HBCs ($K5^{CreERT2}$ mice, selected for TdTomato) and 10,000-67,000 Ascl1 and Neurog1 GBCs (eGFP+) were plated into each well. For the cell-contact transwell experiments, 75,000 cells of HBC-depleted cells were plated on the top chamber. 12,000 HBCs were plated on the bottom chamber or mixed in with the HBC-depleted cells. For the final chamber well experiment, either 75,000 of the HBC-depleted cells were plated, or 12,000 HBCs were additionally added to this population for the positive control.

For the reconstitution experiments, 1:1 and 1:5 mixing ratios of HBCs to Ascl1-GBCs were tested and yielded no statistically different results $p=0.48$. For Neurog1-GBC reconstitution experiments, a 1:5 ratio was used.

Aging experiments used CD1 mice and were plated at a concentration of 75,000 cells/ well of an 8-well chamber slide. The methimazole experiments also used CD1 mice, but loading per well was determined using a dilution curve between 25,000 to 100,000 cells/well depending on the day after methimazole.

Growth media: DMEM/F12 (Gibco #11320-33) was supplemented with recombinant murine R-spondin 1 (200 ng/ml, Prepotech #315-32); recombinant murine Noggin (100 ng/ml, Prepotech #250-38); recombinant murine Wnt-3a (50 ng/ml, Peprotech #315-32); Y27632 (10 µM, TOCRIS #1254); N2 (1%, Gibco #17502-048); B27 (2%, Gibco #17504-044); GlutaMAX 100x (1% vol/vol, Gibco #35050-061); HEPES 1M (10 mM, Gibco #15630-080); Cultrex Stem Cell Qualified Reduced Growth Factor Basement Membrane Extract (4% vol/vol with 9mg/ml of protein, Bio-techne #3434-005-02). [17]. Media was gently changed every other day, with care taken not to aspirate the Cultrex gel that forms on the bottom of the well.

Single-cell RNAseq

Chamber wells containing organoids were washed with ice-cold PBS and dissociated using TrypLE and Dispase until a single-cell suspension was achieved. Single-cell RNAseq libraries were generated using the Evercode WT Mini v2 kit (Parse #ECW02010) following manufacturer instructions. Libraries were sequenced using a Novaseq with a PE200 kit, cycles distributed as R1:146, I1:6, and R2:86. FASTQ files were processed using the Parse bioinformatics pipeline and then analyzed using Scanpy [36]. Standard filtering of min_genes=200 and min cells=2 was performed, and doublets were removed using Scrublet [37]. FASTQ files and processed read counts are deposited at GEO accession: GSE257536. A reviewer token is provided for reviewer access: ohavceeshxybfcn

Immunofluorescence

On D7 of culture, wells were washed with cold 1x PBS and fixed for 5 minutes with 4% PFA (made in 1x PBS, pH 7.2 to 7.3), washed with 1x PBS followed by 15 minutes incubation with PBST (1x PBS, 0.05% Tween 20). Primary antibodies were incubated for 1h at RT or overnight at 4ºC with gentle agitation, followed by 3 washes of PBST and incubation with secondary antibodies for an hour at RT. Table 1 shows the primary and secondary antibody dilutions in blocking buffer (1X PBS, 1% BSA, 0.3% Triton). The slides were mounted in fluoromont G and kept at 4ºC or -20ºC for more extended storage.

Primary antibodies

Name	**Abbreviation on the paper**	**Host**	**Brand/ reference**	**Target**	**Dilution**
Recombinant Anti-GAP43 antibody [EP890Y]	GAP43	Rabbit	Abcam / ab75810	Immature neurons	1:300
Purified anti-Tubulin β 3 (TUBB3) Antibody (clone TUJ1)	TUJ1	Mouse	Biolegend / 801202	Immature neurons	1:3000
UCHL1/PGP9.5 Polyclonal antibody	PGP	Rabbit	Proteintech / 14730-1-AP	Immature and mature neurons	1:800
SOX2 Monoclonal Antibody (Btjce)	SOX2	Rat	Invitrogen / 14-9811-82	HBCs and multipotent GBCs	1:400
Human/Mouse NeuroD1 Antibody	NeuroD1	Goat	R&D systems / AF2746	GBC INP	1:200
Purified anti-Keratin 5 Polyclonal Chicken Antibody	K5	Chicken	Biolegend / 905904	HBCs	1:2000

Mouse anti-Mash-1	Ascl-1	Mouse	BD bioscience / 556604	Ascl-1 GBCs / gbc TA-OSN	1:100
rat anti-KI67	KI67	Rat	eBioscience / 50245564	Dividing cells	1:200
Rabbit anti-Neurogranin	NRGN	Rabbit	Sigma / AB5620	microvillar cells	1:200
Rabbit anti-BSND	BSND	Rabbit	Abcam / ab196017	ionocytes	1:300
Goat anti-OMP	OMP	Goat	Wako / 544-10001-WAKO	mature OSNs	1:300
Various secondary antibodies		Donkey	Jackson Immuno		1:400 (reconstituted in glycerol)

Data analysis

Images were captured on a Zeiss 880 confocal microscope. Image analysis was performed using FIJI/ImageJ (version 1.53). Image preparation and figure assembly were performed in Adobe Illustrator (v 27.5). Only image brightness and contrast were altered in all photographs and applied to the entire image uniformly. For the % pixel by area, images were initially thresholded using the Otsu algorithm positive images before the calculated settings were reused for all data in a given experiment performed together on a single day. Thresholds were recalculated for each independent replicate.

Numerical data was analyzed using GraphPad Prism 10.1.0. All data was tested for normality distribution using the Shapiro-Wilk test. All datasets passed the normality test and were analyzed using ANOVA, followed by Dunnett's post-hoc test. Statistical difference was considered when $p<0.05$. The results are expressed as median (SE). For the methimazole qRT-PCR data, we used the delta-delta CT method for normalization and plotted the data as log2 fold-change. In certain experiments, we normalized the results, measured as a percentage Tuj1+ area, by the original cell input to control for differences in initial plating densities. These were then scaled by 100,000 to generate arbitrary units (a.u.). This was done for the mixing, contact, and methimazole experiments.

Acknowledgments

We thank Po Kwok-Tse for her extraordinary technical assistance and Woochan Jang for his support and assistance. We also thank Albert Tai, Allen Parmelee, and Stephen Kwok of the David Thorley-Lawson Memorial Flow Cytometry Core Facility (NIH S10OD032201) for assistance. This study was supported by the National Institutes of Health (Project NIDCD R21DC018681-01, and R01DC017869-03), and also in part by the Coordenação de Aperfeiçoamento de Pessoal de Nível Superior - Brasil (CAPES) (Finance Code 001).

Conflict of interest

J.E.S. is a co-founder of Rejuvenos Therapeutics and Rhino Therapeutics. E.H.H is a co-founder of Rejuvenos, and a consultant for Rhino Therapeutics. The authors declare no other competing or financial interests.

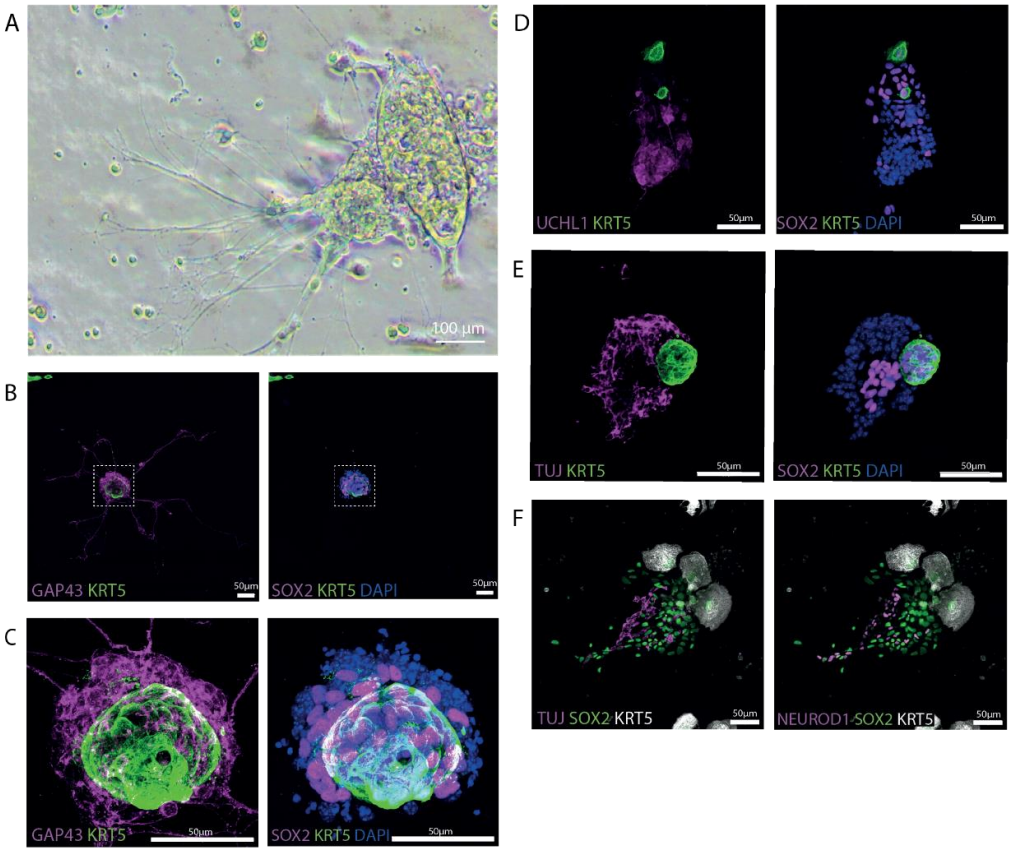
A
100 µm
B
GAP43 KRT5
SOX2 KRT5 DAPI
C
GAP43 KRT5
SOX2 KRT5 DAPI
D
UCHL1 KRT5
SOX2 KRT5 DAPI
E
TUJ KRT5
SOX2 KRT5 DAPI
F
TUJ SOX2 KRT5
NEUROD1 SOX2 KRT5
50µm

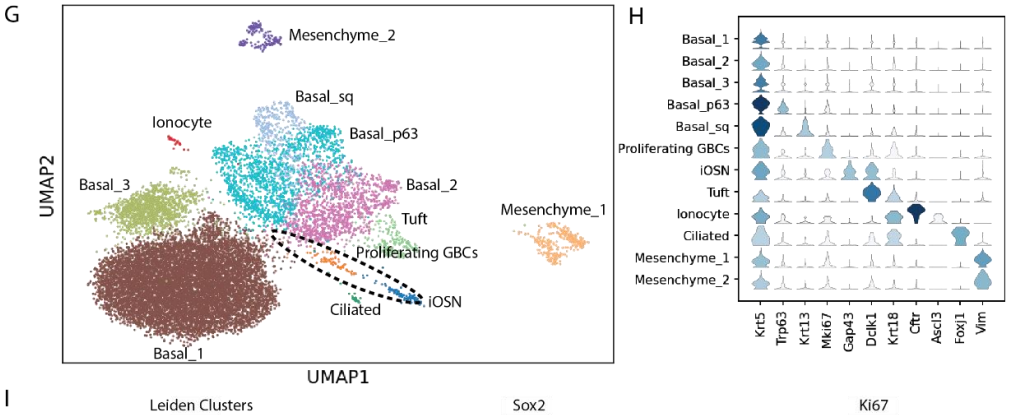
G
Mesenchyme_2
Basal_sq
Ionocyte
Basal_p63
Basal_3
Basal_2
Tuft
Mesenchyme_1
Proliferating GBCs
iOSN
Ciliated
Basal_1
UMAP2
UMAP1
H
Basal_1
Basal_2
Basal_3
Basal_p63
Basal_sq
Proliferating GBCs
iOSN
Tuft
Ionocyte
Ciliated
Mesenchyme_1
Mesenchyme_2
Krt5
Trp63
Krt13
Mki67
Gap43
Dclk1
Krt18
Cftr
Ascl3
Foxj1
Vim

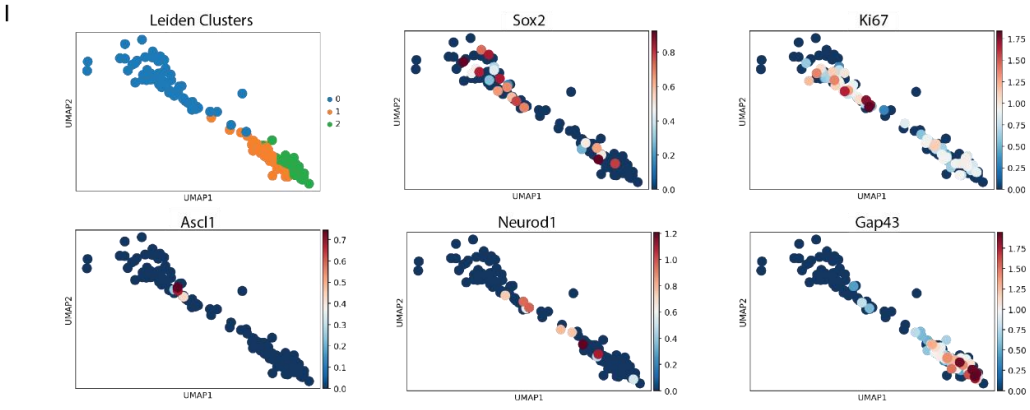
I
Leiden Clusters
Sox2
Ki67
Ascl1
Neurod1
Gap43
UMAP1
UMAP2

Figure 1: Organoid characterization. (A) Representative brightfield of organoid on the seventh day of culture. (B-C) Immunostaining of a representative organoid for iOSNs (Gap43), HBCs (KRT5), and GBCs (SOX2+, KRT5-). C is a high max inset of B. (D-F) Representative immunostaining of organoids for other neurogenic markers. UCHL1 marks all neurons, and NEUROD1 marks immediate neuronal progenitors. (G) UMAP representation of single-cell RNA sequencing of the organoid culture. (H) Stacked violin plots of key marker genes allowing cluster annotation. (I) Focused UMAP expression plots in the dotted area shown in G, representing the neurogenic cascade found in the organoids.

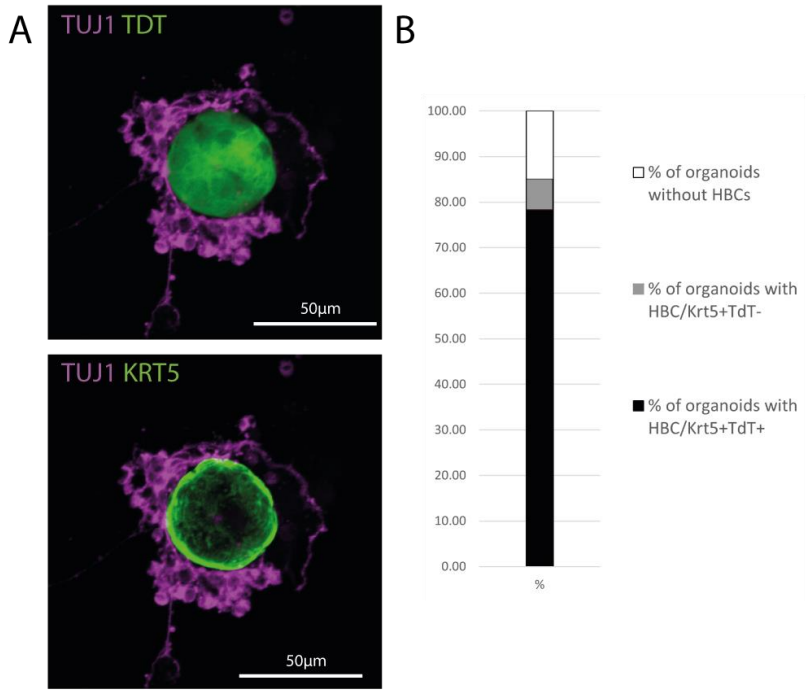

Figure 2: HBC lineage trace. (A) Representative immunostaining of an organoid derived from a KRT5-CreER;LSL-TdTomato lineage trace mouse that was tamoxifen-induced in vivo prior to culture. (B) Percentage of organoids with HBCs labeled and unlabeled with TdTomato. N=9 distinct experiments performed on separate days using different mice.

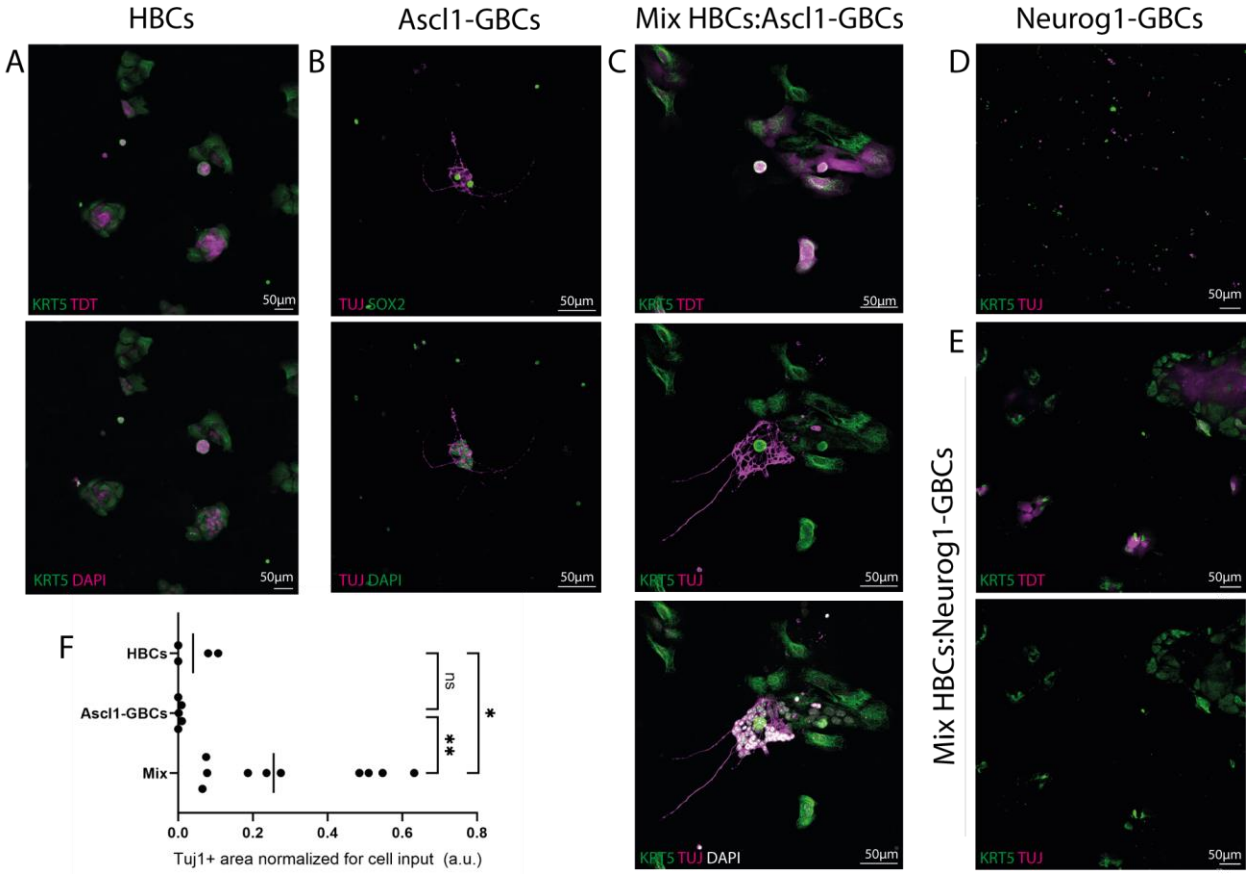

Figure 3: Reconstitution experiments. (A) Immunostaining of HBCs cultured alone; (B) Ascl-1-GBCs alone; (C) HBCs with Ascl1-GBCs; (D) Neurog1-GBCs alone and (E) HBCs and Neurog1-GBCs. (F) Quantification of the Tuj1+ area normalized for cell input (a.u.) of HBCs, Ascl1-GBCs, and the two together. (ANOVA comparison $p=0.0057$,*$p<0.05$,**$p<0.01$) Dots represent distinct biological inputs plated spread over 3 different days using different mice (HBCs=4, Ascl1-GBCs=5, mixture=10).

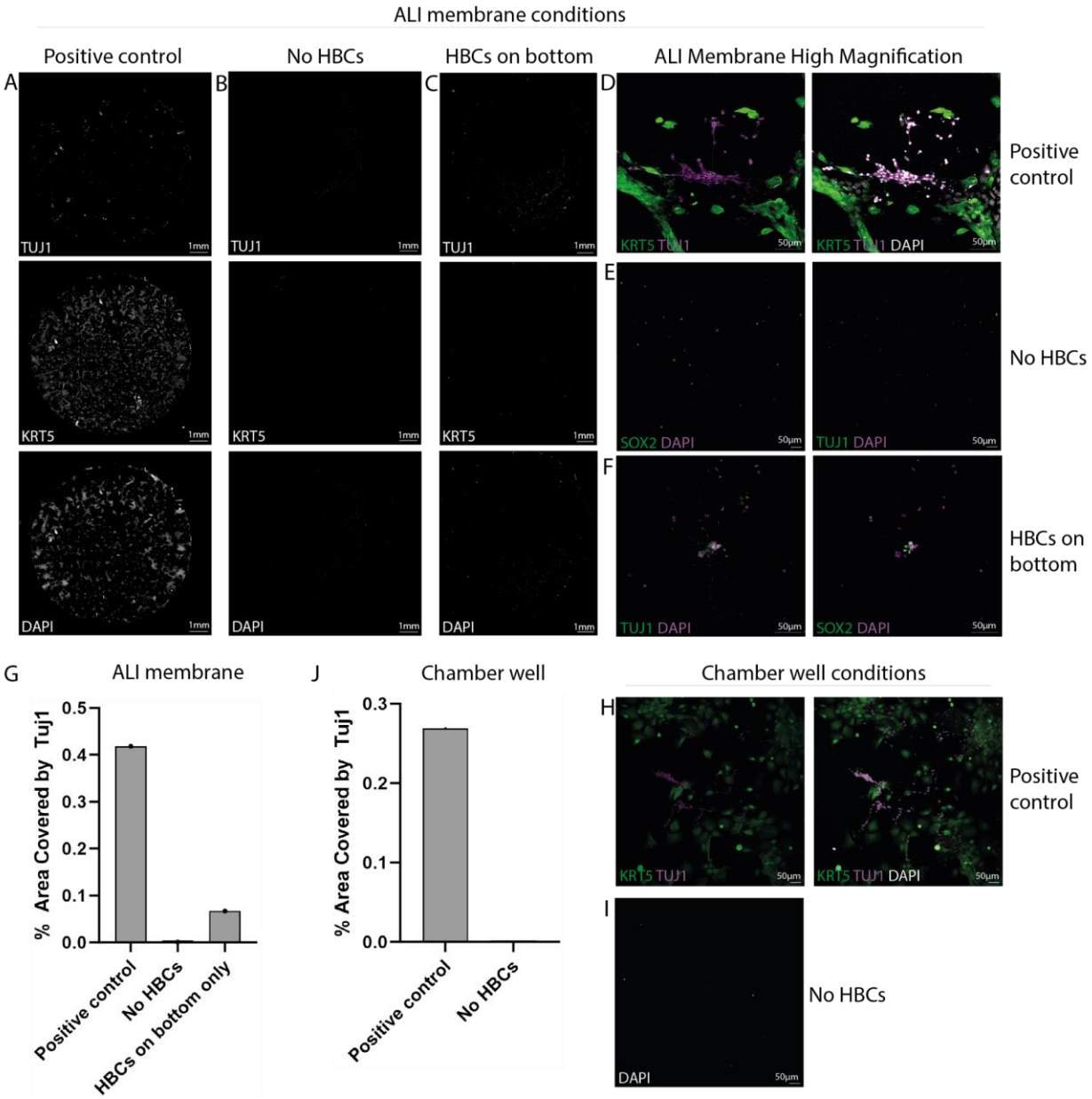

Figure 4: Secretion vs contact-dependency experiments. (A) Immunostaining of entire transwell membranes of positive control (HBCs and negative population reconstituted), (B) HBC depleted, (C) HBCs seeded on the bottom chamber). (D-F) High mag insets of regions shown in A-C. (G) Quantification of the % area covered by Tuj1 in the transwells. (H) Quantification of the % area covered by Tuj1 in the chamber wells. (I) Representative immunostaining of the positive control (reconstituted HBCs and negative population), and (J) the HBC-depleted population seeded into chamber wells as a control. In all HBC-depleted conditions, note the near complete lack of detected signal. Experiments were done on two distinct days, FACS purified from a pool of mice. Two technical replicates each.

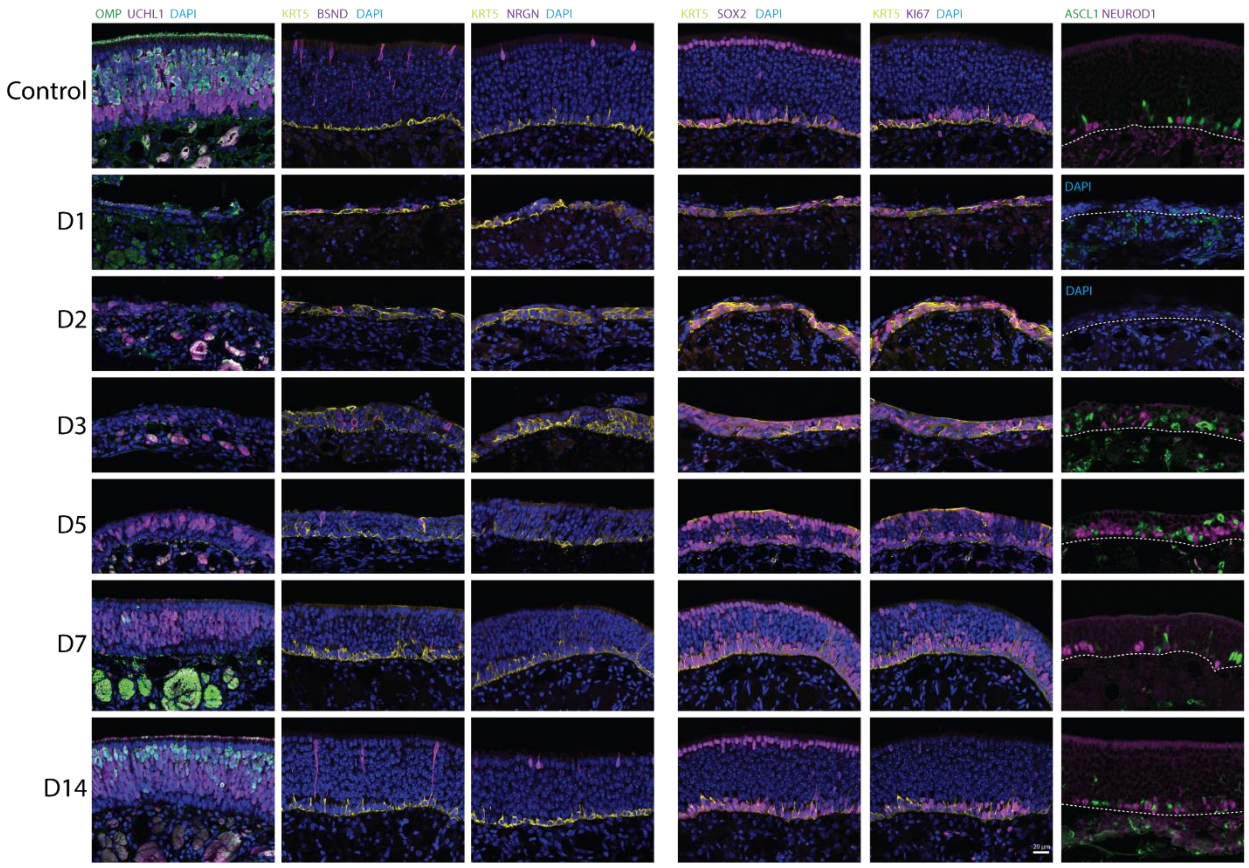

Figure S1. Characterization of methimazole-induced injury. Representative immunofluorescent staining for primary cell types found in the OE in a time course of tissue regeneration after methimazole injury. OMP marks mature OSNs, UCHL1/PGP9.5 marks mature and immature OSNs, KRT5 marks HBCs, BSND marks ionocytes/IP3R3+ microvillar cells, NRGN marks TRPM5+ microvillar/tuft cells, luminal SOX2 marks Sus cells, basal SOX2+ cells that are KRT5- are GBCs, KI67 marks dividing cells, ASCL1 marks neuronally committed upstream GBCs and NEUROD1 marks neuronally committed progenitor GBCs. In the right-most panels, DAPI is omitted except for D1 and D2 post-injury for clarity due to color overlap.

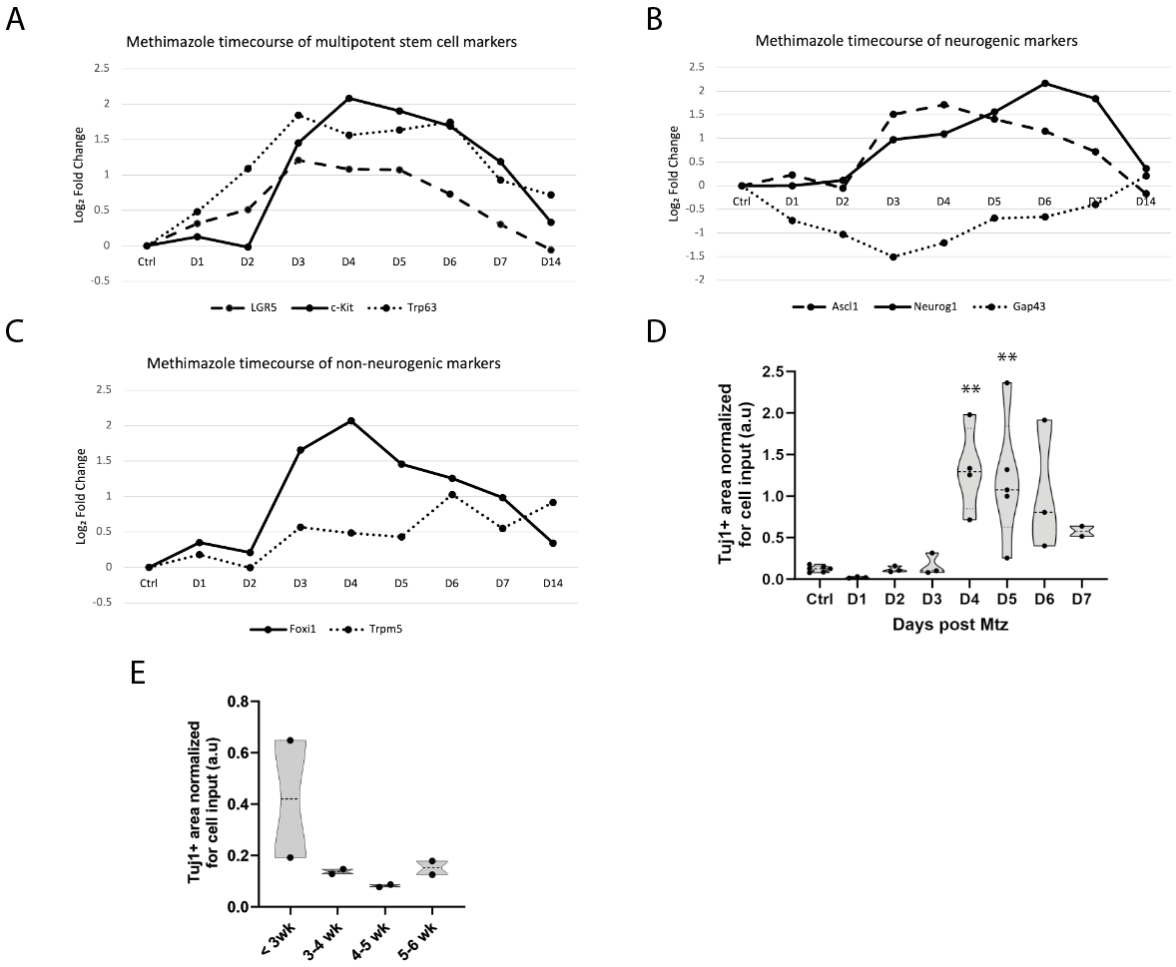

Figure S2. Optimization of the organoid model. q-RT PCR of OE tissue samples collected at time points post methimazole injury, profiling the gene expression of (A) multipotent stem cell markers, (B) neurogenic markers, and (C) non-neurogenic markers relative to control. (D) Quantification of the efficiency of neurogenesis in the organoid system using tissue harvested at different methimazole injury time points, measured as Tuj1+ area normalized for cell input (a.u.). ANOVA comparison $p = 0.001$, $^{**}p < 0.05$ compared to control). (E) Quantification of the Tuj1+ area generated by cells isolated from mice of different ages, normalized for cell input (a.u.). ANOVA comparison $p = 0.298$). qRT-PCR n=1 mouse each timepoint, technical triplicates. Post-Mtz experiments were replicated a minimum of 3 times on distinct mice, with each dot representing a different mouse. Aging experiments were replicated twice, with each dot representing a different mouse.

References

1. Schwob, J.E., Jang, W., Holbrook, E.H., Lin, B., Herrick, D.B., Peterson, J.N., and Hewitt Coleman, J. (2017). Stem and progenitor cells of the mammalian olfactory epithelium: Taking poietic license. J. Comp. Neurol. *525*, 1034–1054.

2. Durante, M.A., Kurtenbach, S., Sargi, Z.B., Harbour, J.W., Choi, R., Kurtenbach, S., Goss, G.M., Matsunami, H., and Goldstein, B.J. (2020). Single-cell analysis of olfactory neurogenesis and differentiation in adult humans. Nat. Neurosci. *23*, 323–326.

3. Child, K.M., Herrick, D.B., Schwob, J.E., Holbrook, E.H., and Jang, W. (2018). The Neuroregenerative Capacity of Olfactory Stem Cells Is Not Limitless: Implications for Aging. J. Neurosci. *38*, 6806–6824.

4. Håglin, S., Bohm, S., and Berghard, A. (2021). Single or Repeated Ablation of Mouse Olfactory Epithelium by Methimazole. Bio Protoc *11*, e3983.

5. Oliva, A.D., Gupta, R., Issa, K., Abi Hachem, R., Jang, D.W., Wellford, S.A., Moseman, E.A., Matsunami, H., and Goldstein, B.J. (2022). Aging-related olfactory loss is associated with olfactory stem cell transcriptional alterations in humans. J. Clin. Invest. *132*. 10.1172/JCI155506.

6. Doty, R.L. (1989). Influence of age and age-related diseases on olfactory function. Ann. N. Y. Acad. Sci. *561*, 76–86.

7. Upadhyay, U.D., and Holbrook, E.H. (2004). Olfactory loss as a result of toxic exposure. Otolaryngol. Clin. North Am. *37*, 1185–1207.

8. Hummel, T., Whitcroft, K.L., Andrews, P., Altundag, A., Cinghi, C., Costanzo, R.M., Damm, M., Frasnelli, J., Gudziol, H., Gupta, N., et al. (2017). Position paper on olfactory dysfunction. Rhinol. Suppl. *54*, 1–30.

9. Holbrook, E.H., Wu, E., Curry, W.T., Lin, D.T., and Schwob, J.E. (2011). Immunohistochemical characterization of human olfactory tissue. Laryngoscope *121*, 1687–1701.

10. Fitzek, M., Patel, P.K., Solomon, P.D., Lin, B., Hummel, T., Schwob, J.E., and Holbrook, E.H. (2022). Integrated age-related immunohistological changes occur in human olfactory epithelium and olfactory bulb. J. Comp. Neurol. *530*, 2154–2175.

11. Jafari, A., and Holbrook, E.H. (2022). Therapies for olfactory dysfunction - an update. Curr. Allergy Asthma Rep. *22*, 21–28.

12. Qian, X., Song, H., and Ming, G.-L. (2019). Brain organoids: advances, applications and challenges. Development *146*. 10.1242/dev.166074.

13. Peterson, J., Lin, B., Barrios-Camacho, C.M., Herrick, D.B., Holbrook, E.H., Jang, W.,

Coleman, J.H., and Schwob, J.E. (2019). Activating a Reserve Neural Stem Cell Population In Vitro Enables Engraftment and Multipotency after Transplantation. Stem Cell Reports *12*, 680–695.

14. Goldstein, B.J., Goss, G.M., Choi, R., Saur, D., Seidler, B., Hare, J.M., and Chaudhari, N. (2016). Contribution of Polycomb group proteins to olfactory basal stem cell self-renewal in a novel c-KIT+ culture model and in vivo. Development *143*, 4394–4404.

15. Chen, M., Tian, S., Yang, X., Lane, A.P., Reed, R.R., and Liu, H. (2014). Wnt-Responsive Lgr5+ Globose Basal Cells Function as Multipotent Olfactory Epithelium Progenitor Cells. J. Neurosci. *34*, 8268–8276.

16. DeHamer, M.K., Guevara, J.L., Hannon, K., Olwin, B.B., and Calof, A.L. (1994). Genesis of olfactory receptor neurons in vitro: regulation of progenitor cell divisions by fibroblast growth factors. Neuron *13*, 1083–1097.

17. Ren, W., Wang, L., Zhang, X., Feng, X., Zhuang, L., Jiang, N., Xu, R., Li, X., Wang, P., Sun, X., et al. (2021). Expansion of murine and human olfactory epithelium/mucosa colonies and generation of mature olfactory sensory neurons under chemically defined conditions. Theranostics *11*, 684–699.

18. Kurtenbach, S., Goss, G.M., Goncalves, S., Choi, R., Hare, J.M., Chaudhari, N., and Goldstein, B.J. (2019). Cell-Based Therapy Restores Olfactory Function in an Inducible Model of Hyposmia. Stem Cell Reports *12*, 1354–1365.

19. Clevers, H. (2016). Modeling Development and Disease with Organoids. Cell *165*, 1586–1597.

20. García-Posadas, L., Arranz-Valsero, I., López-García, A., Soriano-Romaní, L., and Diebold, Y. (2013). A new human primary epithelial cell culture model to study conjunctival inflammation. Invest. Ophthalmol. Vis. Sci. *54*, 7143–7152.

21. Xie, F., Fang, C., Schnittke, N., Schwob, J.E., and Ding, X. (2013). Mechanisms of permanent loss of olfactory receptor neurons induced by the herbicide 2,6-dichlorobenzonitrile: effects on stem cells and noninvolvement of acute induction of the inflammatory cytokine IL-6. Toxicol. Appl. Pharmacol. *272*, 598–607.

22. Li, X., Tong, M., Wang, L., Qin, Y., Yu, H., and Yu, Y. (2020). Age-Dependent Activation and Neuronal Differentiation of Lgr5+ Basal Cells in Injured Olfactory Epithelium via Notch Signaling Pathway. Front. Aging Neurosci. *12*, 602688.

23. Fletcher, R.B., Das, D., Gadye, L., Street, K.N., Baudhuin, A., Wagner, A., Cole, M.B., Flores, Q., Choi, Y.G., Yosef, N., et al. (2017). Deconstructing olfactory stem cell trajectories at single-cell resolution. Cell Stem Cell *20*, 817–830.e8.

24. Bergman, U., Ostergren, A., Gustafson, A.-L., and Brittebo, B. (2002). Differential effects of olfactory toxicants on olfactory regeneration. Arch. Toxicol. *76*, 104–112.

25. Leung, C.T., Coulombe, P.A., and Reed, R.R. (2007). Contribution of olfactory neural stem cells to tissue maintenance and regeneration. Nat. Neurosci. *10*, 720–726.

26. Montoro, D.T., Haber, A.L., Biton, M., Vinarsky, V., Lin, B., Birket, S.E., Yuan, F., Chen, S., Leung, H.M., Villoria, J., et al. (2018). A revised airway epithelial hierarchy includes CFTR-expressing ionocytes. Nature *560*, 319–324.

27. Ualiyeva, S., Lemire, E., Wong, C., Perniss, A., Boyd, A.A., Avilés, E.C., Minichetti, D.G., Maxfield, A., Roditi, R., Matsumoto, I., et al. (2024). A nasal cell atlas reveals heterogeneity of tuft cells and their role in directing olfactory stem cell proliferation. Sci Immunol *9*, eabq4341.

28. Packard, A., Giel-Moloney, M., Leiter, A., and Schwob, J.E. (2011). Progenitor cell capacity of NeuroD1-expressing globose basal cells in the mouse olfactory epithelium. J. Comp. Neurol. *519*, 3580–3596.

29. Krolewski, R.C., Packard, A., and Schwob, J.E. (2013). Global expression profiling of globose basal cells and neurogenic progression within the olfactory epithelium. J. Comp. Neurol. *521*, 833–859.

30. Krolewski, R.C., Jang, W., and Schwob, J.E. (2011). The generation of olfactory epithelial neurospheres in vitro predicts engraftment capacity following transplantation in vivo. Exp. Neurol. *229*, 308–323.

31. Wang H., Deng L., and Qin X. (2023). [Development of an olfactory epithelial organoid culture system based on small molecule screening]. Sheng Wu Gong Cheng Xue Bao *39*, 318–336.

32. Indra, A.K., Warot, X., Brocard, J., Bornert, J.M., Xiao, J.H., Chambon, P., and Metzger, D. (1999). Temporally-controlled site-specific mutagenesis in the basal layer of the epidermis: comparison of the recombinase activity of the tamoxifen-inducible Cre-ER(T) and Cre-ER(T2) recombinases. Nucleic Acids Res. *27*, 4324–4327.

33. Madisen, L., Zwingman, T.A., Sunkin, S.M., Oh, S.W., Zariwala, H.A., Gu, H., Ng, L.L., Palmiter, R.D., Hawrylycz, M.J., Jones, A.R., et al. (2010). A robust and high-throughput Cre reporting and characterization system for the whole mouse brain. Nat. Neurosci. *13*, 133–140.

34. Lin, B., Coleman, J.H., Peterson, J.N., Zunitch, M.J., Jang, W., Herrick, D.B., and Schwob, J.E. (2017). Injury Induces Endogenous Reprogramming and Dedifferentiation of Neuronal Progenitors to Multipotency. Cell Stem Cell *21*, 761–774.e5. 10.1016/j.stem.2017.09.008.

35. Ma, Q., Chen, Z., del Barco Barrantes, I., de la Pompa, J.L., and Anderson, D.J. (1998). neurogenin1 is essential for the determination of neuronal precursors for proximal cranial sensory ganglia. Neuron *20*, 469–482.

36. Wolf, F.A., Angerer, P., and Theis, F.J. (2018). SCANPY: large-scale single-cell gene expression data analysis. Genome Biol. *19*, 15.

37. Wolock, S.L., Lopez, R., and Klein, A.M. (2019). Scrublet: Computational Identification of Cell Doublets in Single-Cell Transcriptomic Data. Cell Syst *8*, 281–291.e9.

CELL PRESS DECLARATION OF INTERESTS POLICY

Transparency is essential for a reader's trust in the scientific process and for the credibility of published articles. At Cell Press, we feel that disclosure of competing interests is a critical aspect of transparency. Therefore, we require a "declaration of interests" section in which all authors disclose any financial or other interests related to the submitted work that (1) could affect or have the perception of affecting the author's objectivity or (2) could influence or have the perception of influencing the content of the article.

What types of articles does this apply to?

We require that you disclose competing interests for all submitted content by completing and submitting the form below. We also require that you include a "declaration of interests" section in the text of all articles even if there are no interests to declare.

What should I disclose?

We require that you and all authors disclose any personal financial interests (e.g., stocks or shares in companies with interests related to the submitted work or consulting fees from companies that could have interests related to the work), professional affiliations, advisory positions, board memberships (including membership on a journal's advisory board when publishing in that journal), or patent holdings that are related to the subject matter of the contribution. As a guideline, you need to declare an interest for (1) any affiliation associated with a payment or financial benefit exceeding $10,000 p.a. or 5% ownership of a company or (2) research funding by a company with related interests. You do not need to disclose diversified mutual funds, 401ks, or investment trusts.

Authors should also disclose relevant financial interests of immediate family members. Cell Press uses the Public Health Service definition of "immediate family member," which includes spouse and dependent children.

Where do I declare competing interests?

Competing interests should be disclosed on this form as well as in a "declaration of interests" section in the manuscript. This section should include financial or other competing interests as well as affiliations that are not included in the author list. Examples of "declaration of interests" language include:

> "AUTHOR is an employee and shareholder of COMPANY."
> "AUTHOR is a founder of COMPANY and a member of its scientific advisory board."

NOTE: Primary affiliations should be included with the author list and do not need to be included in the "declaration of interests" section. Funding sources should be included in the "acknowledgments" section and also do not need to be included in the "declaration of interests" section. (A small number of front-matter article types do not include an "acknowledgments" section. For these articles, reporting of funding sources is not required.)

What if there are no competing interests to declare?

If you have no competing interests to declare, please note that in the "declaration of interests" section with the following wording:

> "The authors declare no competing interests."

August 1, 2023

CELL PRESS DECLARATION OF INTERESTS FORM

If submitting materials via Editorial Manager, please complete this form and upload with your initial submission. Otherwise, please email as an attachment to the editor handling your manuscript.

Please complete each section of the form and insert any necessary "declaration of interests" statement in the text box at the end of the form. A matching statement should be included in a "declaration of interests" section in the manuscript.

Institutional affiliations

We require that you list the current institutional affiliations of all authors, including academic, corporate, and industrial, on the title page of the manuscript. ***Please select one of the following:***

☒ All affiliations are listed on the title page of the manuscript.

☐ I or other authors have additional affiliations that we have noted in the "declaration of interests" section of the manuscript and on this form below.

Funding sources

We require that you disclose all funding sources for the research described in this work. ***Please confirm the following:***

☒ All funding sources for this study are listed in the "acknowledgments" section of the manuscript.*

*A small number of front-matter article types do not include an "acknowledgments" section. For these, reporting funding sources is not required.

Competing financial interests

We require that authors disclose any financial interests and any such interests of immediate family members, including financial holdings, professional affiliations, advisory positions, board memberships, receipt of consulting fees, etc., that:

(1) could affect or have the perception of affecting the author's objectivity, *or*
(2) could influence or have the perception of influencing the content of the article.

Please select one of the following:

☐ We, the authors and our immediate family members, have no financial interests to declare.

☒ We, the authors, have noted any financial interests in the "declaration of interests" section of the manuscript and on this form below, and we have noted interests of our immediate family members.

Advisory/management and consulting positions

We require that authors disclose any position, be it a member of a board or advisory committee or a paid consultant, that they have been involved with that is related to this study. We also require that members of our journal advisory boards disclose their position when publishing in that journal. ***Please select one of the following:***

☐ We, the authors and our immediate family members, have no positions to declare and are not members of the journal's advisory board.

☒ The authors and/or their immediate family members have management/advisory or consulting relationships noted in the "declaration of interests" section of the manuscript and on this form below.

Patents

We require that you disclose any patents related to this work by any of the authors or their institutions. ***Please select one of the following:***

☐ We, the authors and our immediate family members, have no related patents to declare.

☒ We, the authors, have a patent related to this work, which is noted in the "declaration of interests" section of the manuscript and on this form below, and we have noted the patents of immediate family members.

Please insert any "declaration of interests" statements in this space. This exact text should also be included in the "declaration of interests" section of the manuscript. If no authors have a competing interest, please insert the text, "The authors declare no competing interests."

J.E.S. is a co-founder of Rejuvenos Therapeutics and Rhino Therapeutics. E.H.H is a co-founder of Rejuvenos, and a consultant for Rhino Therapeutics. The authors declare no other competing or financial interests.

☒ **On behalf of all authors, I declare that I have disclosed all competing interests related to this work. If any exist, they have been included in the "declaration of interests" section of the manuscript.**

STEM CELL REPORTS

MANUSCRIPT NAME:

MANUSCRIPT NUMBER:

Click here to download full Standards document

Reporting Practices for Publishing Results with Human Pluripotent and Tissue Stem Cells

This checklist is intended to help authors prepare and assess manuscripts for inclusion of critical details relevant to work with human pluripotent stem cells (PSCs) and tissue stem cells (TSCs) with the goal of increasing the rigor and reproducibility of research through reporting.

As of 1 October 2023, each manuscript that includes research with human pluripotent or tissue stem cells is required to include a completed checklist, "Reporting Practices for Publishing Results with Human Pluripotent and Tissue Stem Cells." This document is intended to ensure your manuscript includes pertinent experimental details that will eventually enable the reviewers, and ultimately the readers, to critically evaluate the data and the conclusions. All relevant sections should be filled out with the page number(s) of the manuscript where the details can be found. Sections of the document that are not relevant should be filled out with a "NR." For papers not including work with human stem cells (i.e. papers exclusively using animal-derived stem cells, papers reporting in vivo or in silico work), authors should fill in "NA" in all fields. Detailed supporting information on each section can be found by referring to the reference section in the adjacent column.

During this six-month trial process, the information collected will be used for internal purposes only and will not be sent to reviewers or considered in the decision. After the trial process has ended, the journal anticipates formally implementing this checklist as part of the formal review process. For additional context, please **see the editorial** by Martin Pera, Editor-in-Chief of *Stem Cell Reports*.

	Reference Section	Page Reported in Manuscript
Metadata		
Describe the source of the cells / cell line including:		
Name (or names) / alias of line	1.4; 5.1.2	NR
Unique ID / Registry # (name of registry)	1.4	NR
Source (vendor and catalogue number if obtained commercially); biopsy site and derivation details (if derived)	4.1.1; 5.1	NR
Additional metadata as applicable (e.g., sex, ethnicity, disease information, known mutations, etc.)	4.1.2; 5.4.1	NR

Culture Details		
Describe methods used for isolation, maintenance, and preservation of the cells including:		
Passaging / dissociation / split ratio	3.2; 4.2.2; 5.1.1	NR
Freezing and thawing	5.1.1	NR
Culture reagents used (e.g., media, matrices, growth factors, etc.) with vendor and catalogue number	4.2.2; 5.1.1	NR
The passage number of the cryopreserved / characterized Master Cell Bank or Working Cell Bank stocks used, and the number of subsequent passages prior to and during experimentation	1.2; 3.2.2; 5.1.1	NR

Basic Characterization		
Describe the assessment of the following including when they were performed relative to the experiments:		
Authentication	1.3 ; Appendix 1	NR
Mycoplasma	1.6 ; Appendix 1	NR
Sterility (bacteriostasis / fungistasis)	1.6; Appendix 3	NR

	Reference Section	Page Reported in Manuscript
Genomic Characterization		
Describe the genomic characterization including:		
Methodology used including sufficient detail to allow an assessment of sensitivity (e.g. the number of cells analyzed / resolution / depth of analysis)	3.1; 5.3 ; Appendix 5	NR
Timing of analysis in relation to key experiments reported	3.2	NR
Characterization of Pluripotency and the Undifferentiated State (PSCs only)		
Describe the following:		
Assay methodology	2.1; 2.2; 5.2; Appendix 4	NR
Quantitative results along with statistical analysis	2.1; 2.2; 5.2; Appendix 4	NR
Timing of analysis in relation to key experiments reported	2.1; 2.2; 5.2	NR
Confirmation of cell type (TSCs only)		
Describe the characterization of the following:		
The starting population(s) with recognized markers and methods	4.1; 4.3.1; 5.4.1	NR
Phenotype of expanded cells	4.1; 4.3.1; 5.4.1	NR
Demonstration of lineage potential	4.1; 4.3.1	NR
Molecular Characterization		
Describe the following:		
Confirmation of disease mutation (if applicable)	4.3.4	NR
Confirmation of genetic modification (if applicable)	4.4.3; 4.4.4	NR
Experimental Details		
Describe the following:		
Information regarding the experimental unit or sample type for each experiment (e.g. individuals, cell lines, clones, tissues, organoids, devices, batches, cells, etc.)	4.4.4; 5.4.2	NR
Number and type of replicates	4.2.2; 5.4.2	NR
Data Practices		
Information on:		
Statistical methods used	4.4.1; 5.4.2	NR
Inclusion of the data and annotation code / software used for phenotype classi cation for computationally derived classifiers (if applicable)	5.4.4	NR
Verification that FAIR (https://www.go-fair.org/fair-principles/) and CARE (https://www.gida-global.org/care) data management principles were followed	5.4.4	NR

Additional Comments

All experiments done on murine tissue and cells.